Renewable Energy 256 (2026) 124039

Contents lists available at ScienceDirect

Renewable Energy

journal homepage: www.elsevier.com/locate/renene

Unlocking the energy decarbonization potentials of rooftop photovoltaic-thermal collectors: A case study of Tarragona province's residential communities

Adedamola B. Shobo *, Raul Saez, Dieter Boer, Manel Vallès

Department of Mechanical Engineering, Universitat Rovira i Virgili, Carretera de Valls, S/N, Tarragona, 43007, Spain

ARTICLE INFO

Keywords:
Building rooftop
Domestic hot water
Energy decarbonization
Photovoltaic-thermal collector
Residential energy community
Solar energy

ABSTRACT

The residential sector is a major contributor to global energy demand and carbon emissions, underscoring the need for scalable decarbonization strategies. This study assesses the technical, economic, and environmental potential of deploying simplified rooftop hybrid photovoltaic-thermal (PV-T) collectors across residential communities in Tarragona Province, Spain. Using high-resolution hourly simulation and an energy community framework, the analysis covered 184 municipalities with annual solar irradiation ranging from *1599.4* to 1804.1 kWh/m^2/yr.

Flat-box, water-based PV-T collectors connected directly to municipal water supplies were modeled without auxiliary storage or pumping systems. Results show that with just *3.85 %* rooftop surface occupancy (*0.125 m^2/capita*), the proposed configuration can meet *11.8 %* of the domestic hot water (DHW) energy and *1.8 %* of the electricity demand collectively in the province, delivering *808.4 - 896.9 kWh$_{th}$/m^2* and *233.0 - 259.6 kWh$_e$/m^2* annually across the municipalities. The proposed integration of PV-T collectors economically attractive, achieving a payback of *5 - 6* years, net present values (NPV) of *€1485.82 - €1755.86/m^2,* and a levelized cost of exergy (LCOEx) between *8.43 - 9.95 c€/kWh* across the municipalities. Environmentally, the installations could mitigate approximately *29.3 ktCO$_2$-eq* annually, at a specific avoidance cost of *€13.80/tCO$_2$-eq*.

These findings demonstrate that simplified integration of rooftop PV-T collectors offer a cost-effective and replicable pathway for decarbonizing energy use in the residential sector.

1. Introduction

The residential sector accounts for approximately *30 %* of global energy and contributes about *26 %* of global carbon emissions [1]. Addressing climate change and reducing energy poverty requires urgent efforts to increase the adoption of renewable energy sources and enhance energy efficiency within this sector [2]. A crucial step in accelerating the transition to low-carbon energy is identification and quantification of available renewable energy resources in specific locations, along with the exploration of the strategies to optimize their utilization [3]. Solar energy, in particular, has shown significant potential to replace fossil fuels across various energy applications, yet its practical adoption still lags behind its theoretical potential [4]. Among the mature technologies for harnessing solar energy, rooftop systems such as photovoltaic (PV), solar thermal, and hybrid photovoltaic-thermal (PV-T) collectors offer distinct advantages, including land conservation, self-consumption of generated energy, and the promotion of zero- or positive-energy buildings [5]. Hybrid PV-T collectors, which simultaneously generate electricity and thermal energy, present a promising solution for meeting residential energy needs. These systems also improve electrical efficiency by cooling the PV modules, thus extending their operational lifespan [6]. Despite these benefits, the adoption of PV-T collectors has remained limited within the renewable energy sector [7,8]. Huide et al. [9] demonstrated that integrating rooftop PV-T collectors into residential energy systems can significantly increase the solar contribution to the total energy consumption in both rural and urban settings. In their review, Herrando et al. [10] estimated that widespread adoption of PV-T technologies could reduce global emissions by approximately *16 %* by *2030*. The authors further emphasized the importance of exploring water-based PV-T systems for domestic hot water and space heating, coupled with comprehensive life cycle and economic assessments, to promote broader adoption.

* Corresponding author.
E-mail address: adetumirola@gmail.com (A.B. Shobo).

https://doi.org/10.1016/j.renene.2025.124039
Received 9 June 2024; Received in revised form 12 July 2025; Accepted 19 July 2025
Available online 20 July 2025
0960-1481/© 2025 The Authors. Published by Elsevier Ltd. This is an open access article under the CC BY license (http://creativecommons.org/licenses/by/4.0/).

Several studies have investigated the performance of rooftop, water-based, flat-plate PV-T collectors for providing domestic hot water energy in residential buildings across various climates. Abdul-Ganiyu et al. [11] compared the performance of rooftop-mounted PV and flat-box, water-based PV-T collectors in a residential building in Ghana. The study found that the PV-T system delivered *107 %* more total exergy per unit area and had a *26 %* lower levelized cost of exergy than the PV collector over a *25*-year period. Similarly, Hazami et al. [12] reported that a flat-box, water-based PV-T collector in Tunisia could meet *14.6 %* of the annual hot water needs and *5.3 %* of the annual electricity demand for a residential building. The system also offered greater lifetime financial savings compared to standalone PV and solar thermal collectors. Behzadi et al. [13] demonstrated that an optimized smart residential energy system with integrated PV-T collectors in Denmark could reduce CO_2 emissions by 220 kg/MWh and lower energy costs by *16.7 €/MWh* for electricity and by *7.7 €/MWh* for hot water energy needs. Aguilar-Jiménez et al. [14] conducted a techno-economic analysis of PV-T collector-coupled energy system for use in residential building at five locations: Madison (USA), Soria (Spain), Fresno (USA), Bigene (Guinea-Bissau), and Mexicali (Mexico). The results revealed annual solar thermal fractions ranging from *0.27* to *0.47* respectively, and Soria emerged as the most economically attractive location, featuring a system payback of *9* years. In contrast, the payback at Fresno was *14* years and at both Mexicali and Begene was *18.5* years, while the investment on installation at Madison would not be recovered by the end of the system's lifespan. Other researchers have explored the optimization of building energy systems through the integration of water-based PV-T collectors with other complementary technologies. Herrando et al. [15] presented a study in which water-based PV-T collectors were combined with a heat pump and two hot water storage tanks to meet the heating, cooling and power needs of a building in Zarragoza, Spain. This integrated system resulted in a *50 %* lower environmental impact compared to grid-based systems, and *20 %* less than conventional PV-based systems for the same end uses. Expanding on this, Krakon et al. [16] investigated a novel hybrid system coupling water-based PV-T collectors with heat pump, hot water storage tank, and a biodigester-fed burner for a residential building in Norway. The study demonstrated that the PV-T collector could supply up to *64.8 %* of the space cooling energy in the summer and over *80 %* of the annual DHW energy needs.

However, critical limitations across most of the previous studies include: (a) focus on individual residential buildings, with limited attention given to community- or municipal-scale deployment; (b) failure to present holistic view integrating technical, economic, and environmental benefits across broader populations; (c) heavy reliance on complex configurations involving thermal energy storage tanks and electrical pumps, which increased cost and limited scalability; and (d) reliance on constant water inlet temperatures and average solar irradiation, despite their temporal variations which would affect system performance in reality. Osman [17] emphasized that the high upfront investment in new renewable energy infrasructure poses a significant barrier to achieving global net-zero emissions goals. Herrando, Ramos, and Zabalza [8] echoed this concern, stressing the need to reduce the capital costs of solar-integrated cooling, heating, and power systems to enhance their market viability.

The energy community model, which is a distributed generation/consumption approach, can facilitate collective ownership and operation of renewable energy systems. Parreño-Redriguez et al. [18] suggested that such a model offers a promising pathway to more inclusive and efficient renewable energy adoption.

This study aims to address the dual challenges of high upfront costs and limited community-scale evaluation of PV-T systems. Specifically, it investigates the techno-economic and environmental feasibility of deploying rooftop water-based PV-T collectors across residential communities in the municipalities of Tarragona province of Spain.

The novelty of this study lies in its simplified, cost-reducing system configuration and community-based modeling approach. While the concept of integrating PV-T collectors into residential energy is not new, this study introduces a cost-effective and scalable approach by eliminating traditional components such as auxiliary thermal energy storage tanks, electrical batteries, pumps, and complex water control mechanisms, which are commonly included in conventional PV-T systems. By removing these components, the proposed configuration in this paper is aimed at reducing the capital costs of integrating PV-T collectors and improve the feasibility of widespread deployment. To ensure the robustness and applicability of this approach, this study utilizes a real-world, data-driven methodology, supported by high-resolution simulations based on demographic, meteorological, and housing stock data. This time-granular analysis ensures that the study's assessments are grounded in realistic conditions, as recommended by Saez et al. [18].

Through this framework, this study provides: (a) estimation of the minimal rooftop area requirement per municipality for PV-T collector installation based on domestic hot water consumption; (b) detailed insights into installation feasibility, paybackperiod, CO_2 emission mitigation, and levelized exergy cost; and (c) strategic guidance for scaling PV-T technology adoption in residential communities. Overall, this study offers a scalable, replicable, and policy-relevant model for accelerating renewable energy transition in the residential sector.

2. Materials and methods

2.1. Physical model

This study proposes the use of flat-plate, water-based photovoltaic-thermal collectors mounted on the rooftops of residential buildings within each municipality. The PV-T collectors are connected to the municipal water supply system, with water flow regulated by photosensitive controllers. These controllers ensure that water flows at a constant rate whenever solar irradiation is available (i.e., when $G > 0$) and halt the flow in the absence of solar irradiation (i.e., when $G = 0$). A schematic diagram of the proposed configuration is shown in Fig. 1, illustrating the hydraulic connections of the PV-T collectors in a parallel array. The water exiting from the PV-T collectors is directed into residential domestic hot water (DHW) boilers for auxiliary heating. Simultaneously, the direct current (DC) electricity produced by the collectors is converted to alternating current (AC) by electrical inverters. The AC electricity is then fed into the municipal electricity supply network, providing power to residential buildings within the community.

The following assumptions were made in this study.

1. That each residential building or dwelling has existing gas-powered DHW boiler installed to which pre-heated water from the PV-T collector flows.
2. That the hydraulic pipes connecting the PV-T collectors to the DHW boilers in the buildings are perfectly insulated and thus, no heat losses.

2.2. Case study

Spain has made significant progress in its energy decarbonization efforts, aiming to achieve a *48 %* renewable energy contribution to its energy mix by *2030* [21,22]. With abundant solar insolation, averaging between *1600* and *3000* h annually across the country, Spain is well-positioned to harness its solar energy resources effectively [23]. Solar photovoltaic technology has seen rapid growth in Spain, with substantial installed capacity [24]. The energy community model, supported by Spain's regulatory frameworks, holds considerable promise for enhancing consumer participation, increasing energy efficiency, and reducing carbon emissions [18,25].

However, detailed studies on the widespread adoption of rooftop PV-T collectors in Spanish residential settings, particularly at municipal or regional scales, remain limited. This case study focuses on the residential communities within Tarragona province, located in northeastern Spain

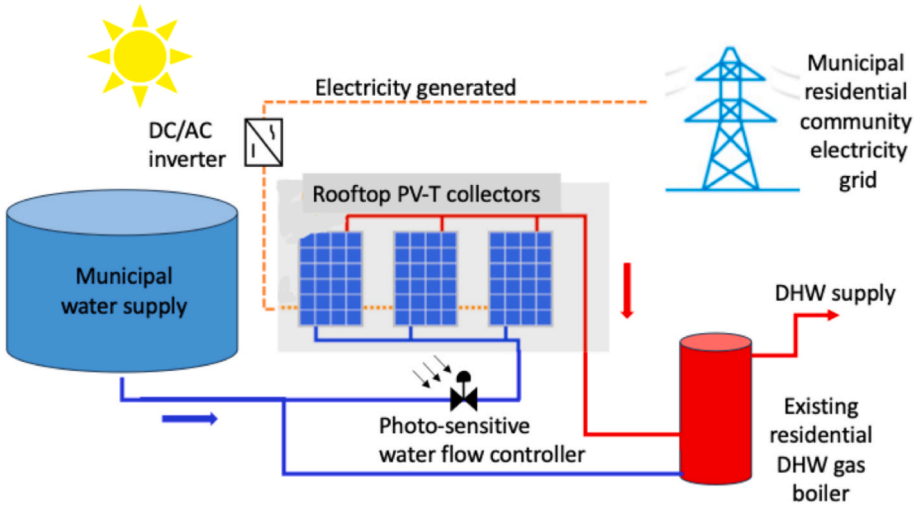


Fig. 1. A schematic of the physical model of the proposed layout considered in this study [20].

(geographical coordinates: *0.25*° - *1.63*°, *40.54*° - *41.56*°) Tarragona experiences Mediterranean climatic conditions, with total annual solar irradiation ranging from *1599.39* to *1804*.05 kW/m^2/yr. Fig. 2 shows the map of Tarragona, highlighting its *184* administrative municipalities.

2.3. Computational approach

The computational framework employed in this study consists of three main components: data acquisition, data processing, and data analysis. The approach is driven by publicly available datasets, ensuring transparency and reproducibility. A schematic diagram of the computational algorithm employed in this study is shown in Fig. 3.

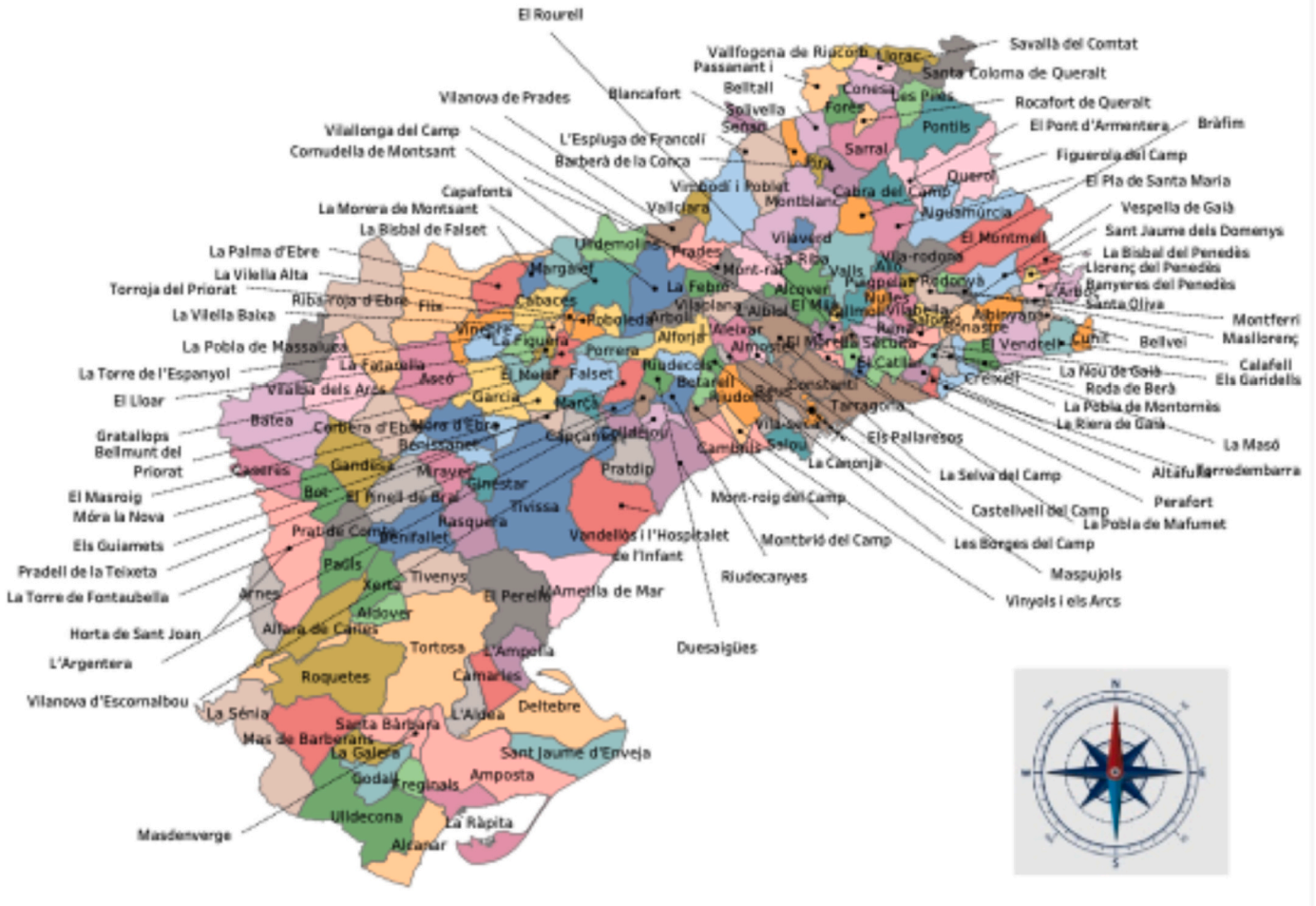


Fig. 2. A map of Tarragona province, showing its constituent municipalities [20].

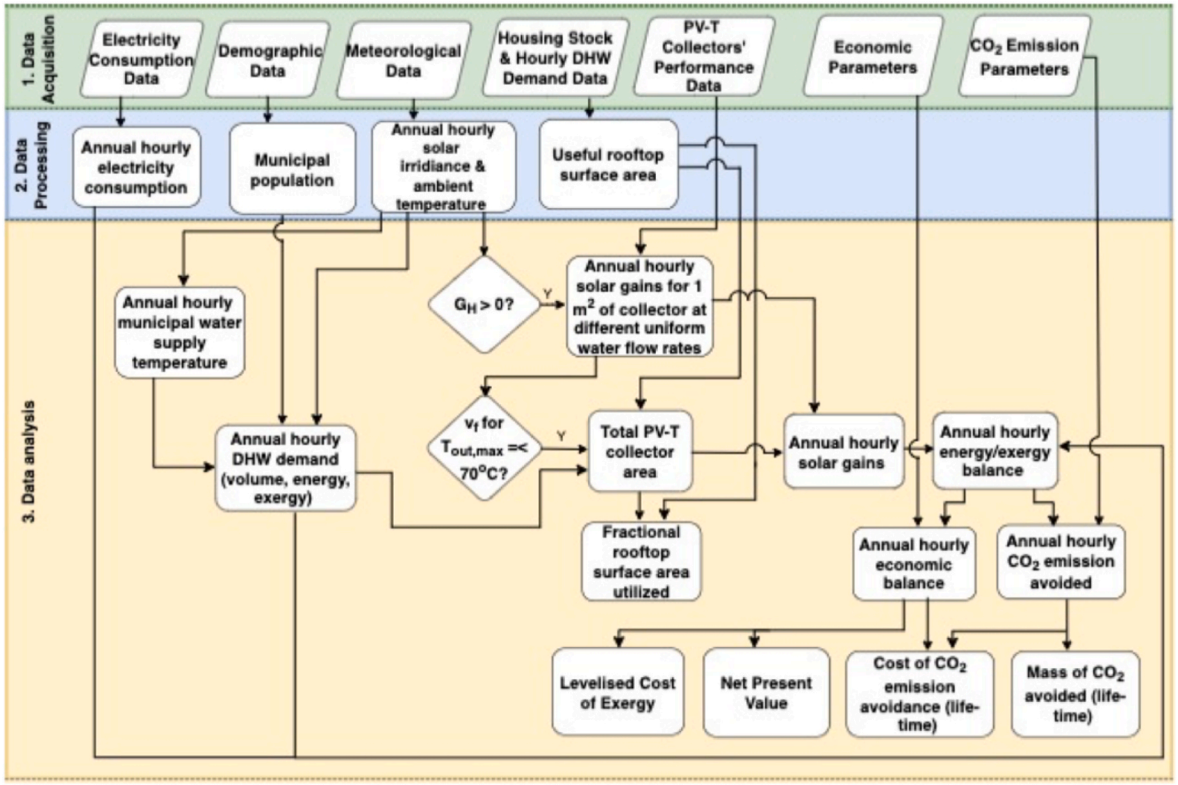


Fig. 3. The algorithm of the solution.

2.3.1. *Electricity consumption, demographic and meteorological data*

The hourly sum of electricity consumption data for all the residential buildings and dwellings in each municipality for the year *2019* was sourced from the Datadis online platform [26]. These data were assumed to represent the typical consumption patterns for the municipalities in this study. Demographic data, including population statistics for *2023*, were sourced from Spanish National Institute of Statistics [27]. The typical meteorological year (TMY) data for each municipality were downloaded from Photovoltaic Geographical Information System (PVGIS) online platform [28]. This data included typical annual hourly solar irradiation and ambient temperature for each municipality, which were filtered and used for the simulations.

2.3.2. *Housing stock and DHW demand profile data*

The total available rooftop space on residential buildings in each municipality was estimated using the data on housing stock characteristics and demographics from the Spanish Ministry of Development and the Statistical Institute of Catalonia [29,30]. A reduction factor of *0.19*, as recommended by the Ministry [29], was applied to account for architectural constraints such as voids, recesses, chimneys, and air-conditioning equipment, and shading effects from surrounding buildings. The methodology for estimating the rooftop space was outlined in Ref. [31]. Hourly DHW demand profiles were sourced from the Spanish Ministry of Transport, Mobility, and Urban Agenda [33].

2.3.3. *PV-T collectors' performance data*

The key technical parameters for the flat-box PV-T collector used in this study are summarized in Table 1. These optical, electrical and thermal characteristics determine the performance of the collector. The collector's design is based on a commercially available model by SOL-IMPEKS Solar Corp. [35], whose thermal performance characteristics were experimentally investigated by Sun et al. [34]. It features a copper plate absorber beneath the photovoltaic module, with cylindrical copper pipes attached to its undersides, facilitating heat transfer to the water flowing through. This study adopted multi-crystalline silicon PV module within each collector due to their reported lower lifecycle environmental impacts compared to the mono-crystalline silicon alternatives [36]. A single layer of tempered glass was also assumed as glazing cover to enhance thermal efficiency [37].

Table 1
Technical parameters for the flat-bx PV-T collector considered in this study.

Parameters	Value
PV cell type	Multi-crystalline Silicon
Glazing type	Tempered glass
Number of layers of glazing	1
Optical efficiency of glazing, η_o	0.8
Thermal energy absorber material type	Copper
Electrical efficiency of PV module, η_{STC}	16 % (@STC)
PV module's temperature coefficient, γ	0.37 %/°C
Nominal operating cell temperature (NOCT) for PV cell	45 °C
PV-T module's thermal efficiency factor, F'	0.8446 [34]
PV-T module's heat loss factor, U_L	6.6382 W/(m^2*K) [34]
PV-T collectors' annual performance degradation factor	0.5 % per annum [11]
PV-T collectors' annual losses due to soiling	0.5 % Per annum [38]

2.3.4. *Economic parameters*

Some of the economic parameters employed in this study are outlined in Table 2. These include the costs of the different system components; costs of assembling, operating and maintaining the system; natural gas price; and some national economic parameters.

This study employed the average electricity price (EP) scenario for the Spanish electricity market as presented in Table 3 and a fixed rate of selling electricity to the grid (ES) of *c€* 9/kWh. A fixed selling price was adopted to ensure modeling simplicity and comparability across all municipalities. While real-time dynamic pricing may fluctuate based on time-of-use or policy, the assumed fixed rate provides a conservative and transparent estimate of revenue from exported electricity.

Table 2
The economic parameters for this study.

Parameters	Value
Cost of collector (€//m^2)	250 [9]
Cost of inverters & electrical cables (€//m^2 of collector)	100 [39]
Cost of hydraulic circuit (€//m^2 of collector)	100 [39]
Cost of assembling (€//m^2 of collector)	125 [Assumed]
Cost of O&M (based on cost of collectors)	5 % [11]
Harmonized energy price escalation rate, *e*	7.6 % [40]
Discount rate, *d*	5 % [11]
Natural gas price, *GP* (c€/kWh)	8.91 [41]
Interest rate, *i*	0.16 % [42]

Table 3
Average electricity prices [19].

Hour	0–8	8–10	10–14	14–18	18–22	22–24	Weekends
Cost (*c€/kWh*)	12	18	24	18	24	18	12

2.3.5. CO_2 emission parameters

This study assumed that natural gas boilers are currently used in the residential dwellings for the provision of DHW energy, and that electricity is supplied from the grid. The equivalent CO_2 emission data associated with energy supply from natural gas boilers and the Spanish electricity grid were used to estimate the equivalent CO_2 emission for this study. The emission factors for both sources are presented in Table 4, which were applied in the calculation of the equivalent CO_2 emission avoided by the proposed PV-T installations.

2.4. Data analysis

The data analysis in this study consists of several key steps, including the calculation of thermal and electrical gains from the PV-T collectors, the conversion of energy to exergy, and the evaluation of the economic and environmental impacts.

2.4.1. PV-T collector solar gains

The daily municipal water supply temperature (T_w) was calculated using the model developed by the National Renewable Energy Laboratory, USA [45,46]. For each day, the tap water temperature was assumed to remain constant across all hours. The model is given as:

$$T_w = 1.8\left(T_{a,avg} - 14.44\right) + 64 + \left[Ratio\left(\frac{T_{a,max} - T_{a,min}}{1.11}\right)\sin(0.9863(Day\ No. - 15 - Lag) - 90)\right] \quad (1)$$

where,

$$Ratio = \left(0.4 + 0.018\left(T_{a,avg} - 6.67\right)\right) \quad (2)$$

$$Lag = 35 - \left[1.8\left(T_{a,avg} - 6.67\right)\right] \quad (3)$$

Here, $T_{a,avg}$ (^oC) is the annual average ambient temperature; $T_{a,max}$ (^oC) is the maximum average monthly ambient temperature; $T_{a,min}$ (^oC) is the minimum average monthly ambient temperature; and *Day No.* is the day-of-the-year.

The daily DHW demand was estimated based on a standardized per capita consumption of *0.03* m^3 at *60* °*C* [47]. Therefore, the corresponding quantity of daily DHW energy demand ($E_{DHW,demand}$) per municipality was computed by Ref. [48]:

$$E_{DHW,demand}(J) = 0.03 \cdot Pop \cdot \rho_w \cdot c_w \cdot (60 - T_w)^\circ C \quad (4)$$

where, *Pop* is the municipal population, ρ_w is the density of tap water and c_w is the specific heat capacity of tap water.

The hourly DHW energy demands were then estimated by multiplying the daily DHW energy demand ($E_{DHW,demand}$) by the fractional DHW demand corresponding to each hour according to the hourly distribution of DHW volume demand presented in Fig. 4.

The electrical and thermal gains for the PV-T collectors were obtained by employing the methods outlined in Ref. [34], where nominal operating cell temperature (NOCT) of the PV module for each hour was determined by:

$$NOCT_{PVT} = \left[800F_R\left(\frac{T_w - T_a}{G}\right)\right] + \left[\frac{F_R\eta_o}{F_R U_L}(1 - F_R)800\right] + 20 \quad (1)$$

where, F_R, the PV-T module's heat removal factor was determined by:

$$F_R = \frac{\dot{m}_w c_w}{A_c U_L}\left[1 - exp\left(-\frac{A_c F U_L}{\dot{m}_w c_w}\right)\right] \quad (2)$$

The PV module's average temperature at each hour was then estimated using:

$$T_{PV} = [T_a + (NOCT_{PVT} - 20)]\frac{G}{800} \quad (3)$$

where T_a is the hourly average ambient temperature and *G* is the hourly average solar irradiance.

The electrical efficiency of the PV module was then computed by:

$$\eta_{el,PVT} = \eta_{STC}[1 - \gamma(T_{PV} - T_{STC})] \quad (4)$$

where T_{STC} is the temperature at Standard Testing Condition (STC) which was taken as 25 °C. Therefore, the average electrical energy from PV-T module each hour, was determined by:

$$E_{el,PVT}(kWh) = \frac{GA_c\eta_{el,PVT}}{1000} \quad (5)$$

where A_c is the area of PV-T collector.

The average hourly thermal energy gained by water flowing through the PV-T collector per hour was determined by:

$$E_{th,PVT}(kWh) = \frac{A_c[(F_R\eta_o G) - F_R U_L(T_w - T_a)]}{1000} \quad (6)$$

while the average hourly temperature of water output from PV-T collector was determined by:

Table 4
Equivalent CO_2 emission factors.

Parameters	Value
Emission associated with grid electricity ($kgCO_2$-eq/kWh_e)	0.217 [30,43]
Emission from natural gas boilers ($kgCO_2$-eq/kWh_{th})	0.217 [44]

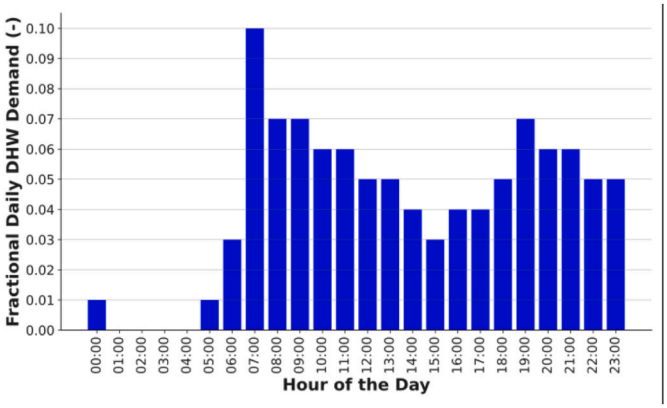


Fig. 4. Hourly distribution of DHW volume demand as a fraction of the total daily demand [33].

$$T_{out}(^{\circ}C) = T_w + \frac{A_c}{\dot{m}_w c_w}[F_R\eta_o G - F_R U_L(T_w - T_a)] \quad (7)$$

where $\dot{m}_w$ is the mass flow rate of water through PV-T collector.

2.4.2. Energy and exergy analysis

Dynamic simulations were performed for each municipality using the typical annual weather data and the calculated hourly municipal water supply temperatures. These simulations involved applying uniform water flowrates of 1 L/min, *0.8* L/min, *0.6* L/min, *0.4* L/min and *0.2* L/min separately tested for each municipality. The flow was activated only during hours with incident solar radiation (i.e., when $G > 0$). The water flowrate maximized thermal gains and maintained outlet water temperature (T_{out}) from PV-T collectors below *70* $^{\circ}C$ throughout the year was selected. The corresponding PV-T collector installation area, A_c, for each municipality was then calculated based on the average hourly DHW demand and a fixed flowrate per unit area. This approach aligns with the approach in Ref. [49], which recommends fixed collector area-to-demand ratio for initial sizing of solar collector area, assuming standardized flowrates. The simplified model yields:

$$A_c = \left[\frac{Average\ hourly\ DHW\ volume\ demand}{Water\ volume\ flow\ through\ 1m^2\ of\ collector\ per\ hour}\right] \quad (8)$$

where,

$$Average\ hourly\ DHW\ volume\ demand = \frac{0.03\ m^3 \times Pop}{24} \quad (9)$$

The hourly DHW thermal energy demands and the hourly thermal energy gains from PV-T collectors were converted to their thermal exergy equivalents by Ref. [50]:

$$Ex_{DHW,demand}(kWh) = E_{DHW}\left(1 - \frac{T_a(K)}{60 + 273(K)}\right) \quad (10)$$

$$Ex_{DHW,PVT}(kWh) = E_{th,PVT}\left(1 - \frac{T_a(K)}{T_{out}(K)}\right) \quad (11)$$

The hourly electrical energy demands, and the electrical energy generated by the PV-T collectors are equated to the corresponding electrical exergies ($Ex_{el,demand}$, $Ex_{el,PVT}$). The exergy approach was utilized for the performance evaluation because it provides more accurate representation of the useful energy produced by the PV-T collectors. Exergy accounts for the quality of energy and its potential to perform useful work. It helps to distinguish between useable thermal energy from losses, which occur due to the temperature gradient between collector and the ambient. The approach also allows for a comprehensive assessment of both useful thermal and useful electrical energy produced. Furthermore, it is crucial for comparing the actual performance of PV-T systems across varying ambient conditions.

The DC/AC electrical inverters in the installations were assumed to operate with at *98 %* efficiency. Energy and exergy balances were then computed for each municipality based on hourly exergy demands (electricity and DHW) and exergy gains from the PV-T collector installations through a typical year.

2.4.3. Economic analysis

The economic viability of the PV-T collector installations was evaluated using the Net Present Value (*NPV*), which accounts for the savings from the PV-T systems for each municipality minus the capital and operational costs. The calculation was performed over a *20*-year period, with the following formula for NPV [51]:

$$\text{Net } Present\ Value\ (NPV) = \sum_{y=0}^{19}\frac{R_y(1+e)^y}{(1+i)^y(1+d)^y} - \left(C_{Capital} + \sum_{y=0}^{19} C_{O\&M}\right) \quad (12)$$

where *20* years was taken as the lifetime of the installations and year of installation was taken as *0*, $C_{Capital}$ is the initial total capital investment of installation, R_y is the annual financial savings expected from the PV-T collectors' installation in the municipality and was calculated based on the methodology by Ref. [39]:

$$R_y = \sum_{h=1}^{8760}\left[\left(EP{\cdot}E_{el,PVT}\right)_{consumed} + \left(ES{\cdot}E_{el,PVT}\right)_{sold} + \left(GP{\cdot}E_{DHW,PVT}\right)_{comsumed}\right] \quad (13)$$

Any excess generated electricity that is not consumed within the energy community each hour was considered exported and sold to external electricity grid while the excess thermal energy/exergy from the PV-T collectors each hour was not catered for.

The levelized cost of exergy (LCOEx) realized from the PV-T collector installations in each municipality, which gives a measure of the cost per unit exergy output of the PV-T installations, was calculated by Ref. [52]:

$$LCOEx = \frac{C_{Capital} + \sum_{y=0}^{19} C_{O\&M}}{\sum_{y=0}^{19}\left(\sum_{h=1}^{8760} Ex_{el,PVT} + \sum_{h=1}^{8760} Ex_{th,PVT}\right)} \quad (14)$$

The cumulative cash flow for each year was computed by Ref. [53]:

$$Cummulative\ Cashflow_y = \sum_{y=0}^{y} R_y - \left(C_{Capital} + \sum_{y=0}^{y} C_{O\&M}\right) \quad (15)$$

It should be noted that to account for the degradation of the PV-T panels over time, *0.5 %* annual degradation factor was applied to the energy generation for each year. This factor, as presented in Table 1, reduces the system's efficiency and output annually. Therefore, the annual energy generation and corresponding financial savings were adjusted to account for this degradation. This ensures that the economic analysis reflects the expected performance reduction over the *20*-year lifetime of the PV-T installations.

2.4.4. CO_2 emission and mitigation analysis

The annual mass of equivalent CO_2 emissions associated with electricity and DHW consumption in the residential communities across municipalities was calculated following the methodology outlined by Ref. [54]. Specifically, the CO_2 emissions from electricity consumption were determined by multiplying the emission factor of electricity supply from the grid (*217.37 kgCO_2-eq/kWh*) by the total annual electricity demand across all hours. Similarly, the CO_2 emissions from DHW consumption were determined by multiplying the emission factor of electricity supply from the grid (*271.00 kgCO2-eq/kWh*) by the total annual electricity demand. Thus, the total annual mass of equivalent CO_2 emissions from both electricity and DHW consumption was computed as:

$$M_{CO_{2,Demand}} = \left(217.37 \cdot \sum_{h=1}^{8760} E_{el,demand}\right) + \left(271.00 \cdot \sum_{h=1}^{8760} E_{DHW,demand}\right) \quad (15)$$

To estimate the annual mass of equivalent CO_2 emissions mitigated by the PV-T installations, the emission factors for both electricity and DHW consumption were applied to the corresponding exergy outputs from all the installations in each municipality. Thus, the annual mass of equivalent CO_2 emissions mitigated was calculated by summing the emission reductions from both the electrical and thermal exergies produced by the PV-T collectors:

$$M_{CO_2,avoided} = \left(217.37 \cdot \sum_{h=1}^{8760} Ex_{el,PVT}\right) + \left(271.00 \cdot \sum_{h=1}^{8760} Ex_{th,PVT}\right) \quad (16)$$

The specific cost of equivalent CO_2 emissions avoidance afforded by the PV-T collectors deployment in each municipality over their lifetime

was determined by:

$$Specific\ Cost\ of\ CO_2\ emission\ avoidance = \frac{C_{Capital} + \sum_{y=0}^{19} C_{O\&M}}{\sum_{y=0}^{19} M_{CO_2,avoided}} \quad (17)$$

2.5. Simulation implementation and computational workflow

The computational implementation of the model was carried out in two distinct phases. In the first phase, an Excel-based framework was developed to simulate the hourly performance of PV-T collector systems across the *184* municipalities. Hourly ambient temperature and solar irradiance data were obtained from the Typical Meteorological Year (TMY) files for each municipality, combined with municipal population data for year *2023* and electricity consumption data for year *2019*. These data were incorporate into a master Excel workbook, with each municipality assigned a dedicated worksheet. equations (1)–(11) presented in the preceding subsections were embedded as formulas within the first worksheet and automatically propagated across all others. This approach enabled the automatic calculation of several key parameters for each municipality on hourly basis, including: water supply temperature; DHW energy demand; required PV-T collector area; electrical and thermal energy outputs from the PV-T system; useful energy supplied, excess exergy, and rooftop occupancy. In the second phase, a Python script was employed to aggregate and analyze the results generated by the Excel framework. This included computing the annual energy balances, financial metrics (e.g., Net Present Value [NPV], Levelized Cost of Exergy [LCOEx]), cost savings, and CO_2 emission avoided for each municipality. To assess spatial feasibility, the model incorporated municipality-specific estimates of useable residential rooftop area. These estimate were sourced from a previous study by the authors [19] and used to calculate the percentage of the available rooftop area to be occupied by PV-T collectors according to the framework in this study.

This two-phase computational approach provided a detailed, high-resolution analysis of the performance, economic viability, and environmental impact mitigation of the PV-T collector installations across a diverse set of municipalities. The methodology ensures full transparency and reproducibility due of its high-resolution temporal modeling and its use of real-world datasets.

3. Results and discussion

3.1. Validation of PV-T collector model

The PV-T model used in this study was validated against the experimental data provided by Ref. [34], specifically comparing the ambient temperature, the water inlet temperature, the PV module's efficiency, and the solar irradiation data that was presented for Chiang Mai on March 16, 2018. The mean absolute errors for the collector's electricity production and outlet water temperature, averaged over simulation period are presented in Table 5. The results indicate that the PV-T collector model used in this study performs within acceptable limits. This demonstrates the reliability and accuracy of the model for simulation.

3.2. Optimal flowrate selection

To determine the optimal uniform water flowrate for the PV-T collectors, a sensitivity analysis was conducted by varying the inlet flowrate from *0.2* to 1.0 L/min (with increments of *0.*2 L/min), under identical climatic conditions and demand profiles for each municipality. The results, aggregated across the province, are summarized in Table 6. The analysis revealed that as the water higher flow rate increased, the required PV-T installation area decreased, as derived from Equation (8). This was because of the larger volume/mass flow of water per unit while the average hourly volume of DHW demand remained constant.

Table 5
Validation results for the PV-T collector model, with respect to the experimental data from Ref. [32].

Parameter	Error (%)
PV-T electricity production (kWh)	5.2 %
PV-T outlet water temperature (°C)	4.9 %

However, higher inlet water flow rates resulted in lower output water temperatures due to reduced residence time in the collectors, leading to diminished thermal exergy gains. Consequently, the annual DHW exergy, electrical exergy, cost savings, and CO_2 emission avoidance decreased significantly at higher flow rates. As such, the *0.*2 L/min flowrate maximized both thermal and electrical exergy outputs, achieving the highest annual cost savings (*12.84 M€),* and CO_2 emission avoidance (*29.3 ktCO$_2$-eq*). While this flowrate required a larger installation area (*102.*8 km^2*),* it optimized solar energy utilization and provided the best balance of performance, economic viability, and environmental impact mitigation.

3.3. Rooftop occupancy by PV-T collectors

Following the identification of the optimal uniform water flowrate of *0.*2 L/min (*~0.*00333 kg/s), the required PV-T collector area for each municipality was analyzed across the province.

Based on the local DHW volume demands and municipal demographics, this configuration yielded an average PV-T collector installation area of *0.125 m^2*per capita. The percentage of the total useful residential buildings' rooftop surface area occupied by the PV-T collectors varied significantly across the municipalities as illustrated in Fig. 5. These differences were influenced by local parameters such as population size; dwelling topology; the ratio of single-family to multi-family buildings; and the average residential dwelling population density of each municipality. At one end of the spectrum, Vallfogona de Riucorb exhibited the lowest rooftop occupancy, with only *0.67 %* of useful rooftop area required. This municipality had a very low average dwelling population density of about *0.41 persons* per *dwelling* (*pop. = 79, number of dwellings = 192*), suggesting the presence of unoccupied or secondary homes. Additionally, its single-family to multi-family building ratio of *13.22* (*119*:9) contributed to abundant available useful rooftop surface area.

On the opposite end, La Canonja recorded the highest rooftop occupancy, with about 21.33 % of the useful rooftop surface required. The municipality had a significantly higher residential dwelling population density of about *2.23 persons* per *dwelling* (*pop. = 5971, number of dwellings = 2670*) and a much lower ratio of single-to multi-family of *0.2* buildings (*444*:*2223*) This limits the useful rooftop surface area per capita. When aggregated across the entire province, a total of approximately *3.85 %* (*~0.*1 km^2) of the total estimated *2.*7 km^2 of the useable residential buildings' rooftop surface area would be required to support the proposed PV-T collector installations.

Table 6
Performance metrics across the province under different water inlet flowrates.

Inlet Water Flowrate (*L/min*)	PV-T Installation Area (m^2)	Annual DHW Thermal Exergy (***MWh***)	Annual Electrical Exergy (***MWh***)	Annual DHW + Electricity Cost Saved (*M€*)	Annual Mass of Emissions Avoided (*ktCO$_2$-eq*)
0.2	102814.3	6515.2	25494.9	12.84	29.3
0.4	51407.1	2019.3	12996.5	9.35	16.0
0.6	34271.4	939.9	8724.7	7.99	11.0
0.8	25703.6	531.4	6566.9	7.29	8.4
1.0	20562.9	335.8	5265.0	6.85	6.7

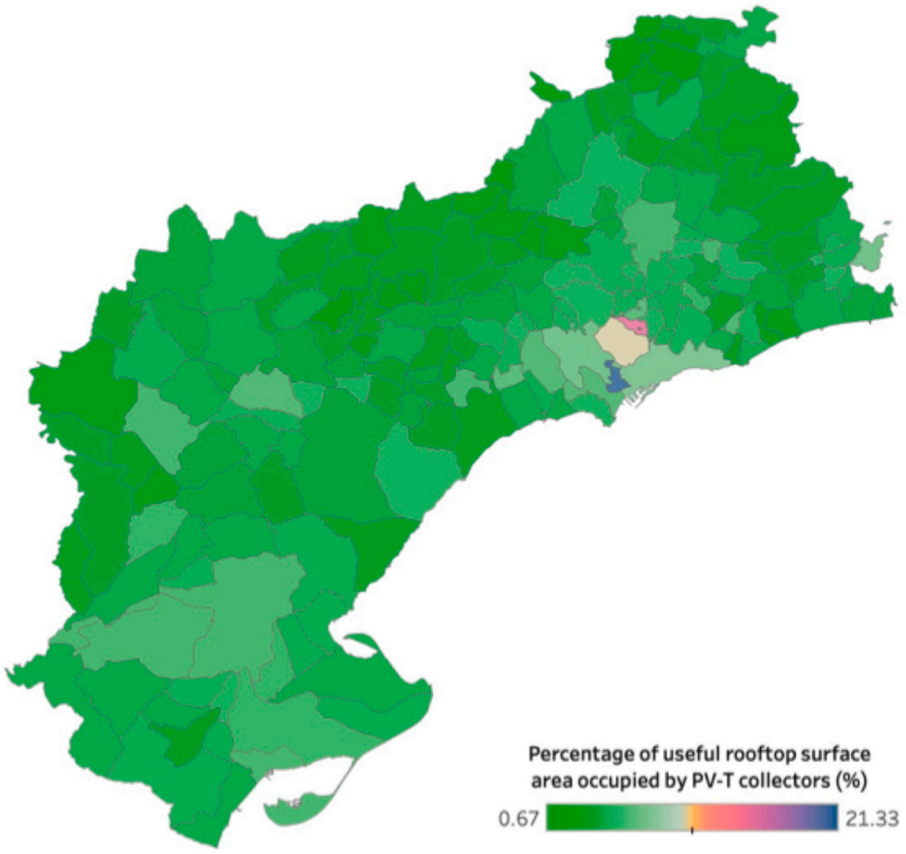


Fig. 5. Percentage of the useful rooftop surface area occupied by PV-T collectors.

3.4. The thermal effects of solar irradiation

The variations in solar irradiance intensity (G) had noticeable impact on both the ambient temperature (T_a) and, consequently, the municipal water supply temperature (T_w). This is clearly demonstrated in Fig. 6(a)–(b), which show the annual profiles for two representative municipalities. Vallfogona de Riucorb, with total annual solar irradiation of approximately *1662.*6 kW/m^2, was chosen for its notably low minimum average monthly ambient temperature ($T_{a,min}$), which was about *2.6* °*C*. In contrast, Caseres, with a slightly higher total annual solar irradiation of *1684.*6 kW/m^2, was selected for its higher maximum average monthly ambient temperature ($T_{a,max}$), which reached about *26.6* °*C*.

As depicted in the figures, the intensity of the solar irradiation (represented in vibrant orange) followed a seasonal pattern, decreasing during winter months and increasing towards the summer. This variation also affected the ambient temperatures (in red) and the municipal water supply temperatures (in dark blue) across the year. The teal line in the graphs tracked the temperature of the water exiting the PV-T collectors for both municipalities, assuming the previously described configuration with uniform water flowrate of *0.*2 L/min. During the winter, when the solar irradiation decreased, the water supply temperature also decreased.

The solar thermal gains by the PV-T collectors ramped up the temperature of the water and this effect can be observed to be increase towards summer because of the greater average solar irradiation. The peak temperature of about *63.8* °*C* was achieved from the PV-T collectors in Vallfogona de Riucorb (at the *5101*th hour) while a maximum of about *66.7* °*C* was achieved in Caseres (at the *4501*th hour). These observations highlight the thermal performance improvements enabled by higher solar irradiation in the warmer months.

The difference in solar irradiation across municipalities resulted in variation in PV-T performance. PV-T collectors in municipalities with higher solar irradiance, like Caseres, generate more thermal and electrical energy, particularly in the summer months. On the other hand, municipalities like Vallfogona de Riucorb, experience decreased energy

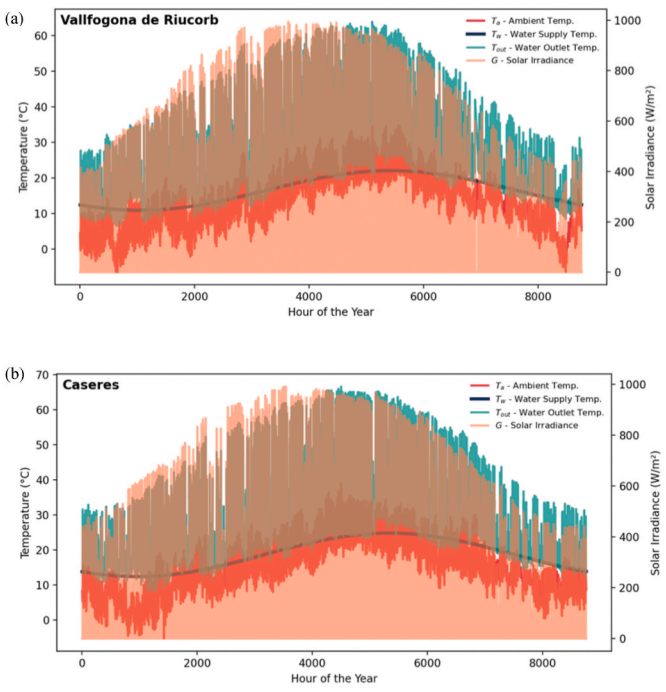


Fig. 6. Annual hourly profiles of the temperatures of the municipal water supply; water outlet from PV-T collectors; and the ambient; with the average solar irradiance for (a) Vallfogona de Riucorb and (b) Caseres.

generation, especially in the winter when solar irradiation is lower. The observed seasonal variations are critical for understanding the system's performance across different municipalities with varying solar resources and climatic conditions.

3.5. Solar fraction afforded by PV-T installations

Fig. 7(a) presents the aggregated annual hourly domestic hot water (DHW) exergy demand and the corresponding exergy provided by the PV-T collectors across all municipalities. The demand profile closely follows seasonal trends solar irradiation, ambient temperature, and water supply temperature as previously illustrated in Fig. 6(a) and (b). During the winter months, lower water supply and ambient temperatures result in higher demand for exergy for heating water. Conversely, during the summer, increased solar irradiation leads to higher thermal gains from the PV-T collectors, reducing the need for additional energy input.

The results show that, on the average, the harnessed energy by the PV-T collectors satisfied approximately *11.8 %* (*~6.52 GWh_{th}*) of the total annual DHW exergy demand (*~55.34 GWh_{th}*) across the province. The solar fraction for DHW consumption varied across the municipalities, ranging from *9.57 %* in Vilanova de Prades to *12.97 %* in Les Borges del Camp. With the proposed configuration, a minimal average of *7.70 %* (*0.54 GWh_{th}*) of the annual thermal exergy generated by the PV-T collectors, aggregated across all the municipalities (ranging from *6.10 %* to *8.86 %*), would be lost due to the mismatch between hourly the DHW volume in demand and the supply from the PV-T collectors.

Fig. 7(b) illustrates the hourly profiles of electricity demand and electricity generated by the PV-T collectors across the province. On the average, the PV-T collectors provide about *1.8 %* (*25.50 GWh_e*) of the total annual hourly electricity demand (*1.40 TWh_e*) across the province. The solar fraction of the electricity consumption varies significantly across the municipalities, from *0.11 %* in La Palma D'Ebre to *7.68 %* in Santa Coloma de Queralt.

The variation in solar irradiation across the municipalities further accentuates this mismatch in energy production. The collectors in the municipalities with higher average solar irradiation, such as Caseres, generate more energy during the summer months. However, larger gaps exist between experience greater gap between energy production and demand during the winter months. In contrast, municipalities with generally lower average solar irradiation, like Vallfogona de Riucorb, face a greater deficit in both DHW and electricity generation year-round. But this issue is pronounced in the winter months. The reduced solar irradiation during winter exacerbates the energy shortfall, making these municipalities more reliant on external energy sources.

Overall, the PV-T installations contributed an average solar fraction of *2.20 %* (ranging from *0.14 %* to *8.06 %*) to the combined annual electricity and DHW exergy consumptions across the province. The annual exergetic potentials of the PV-T collector installations are approximately *63.37 kWh_{th}/m^2* (ranging from *57.00 kWh_{th}/m^2* to *68.01 kWh_{th}/m^2*) for DHW exergy demand, and *247.97 kWh_e/m^2* (ranging from *233.0 kWh_e/m^2* to *259.6 kWh_e/m^2*) for electricity demand.

In energy terms, the PV-T collectors in this study are estimated to provide between *808.4 $kWh_{th}/m^2/yr$ and 896.9 kWh_{th}/m^2*/yr for DHW

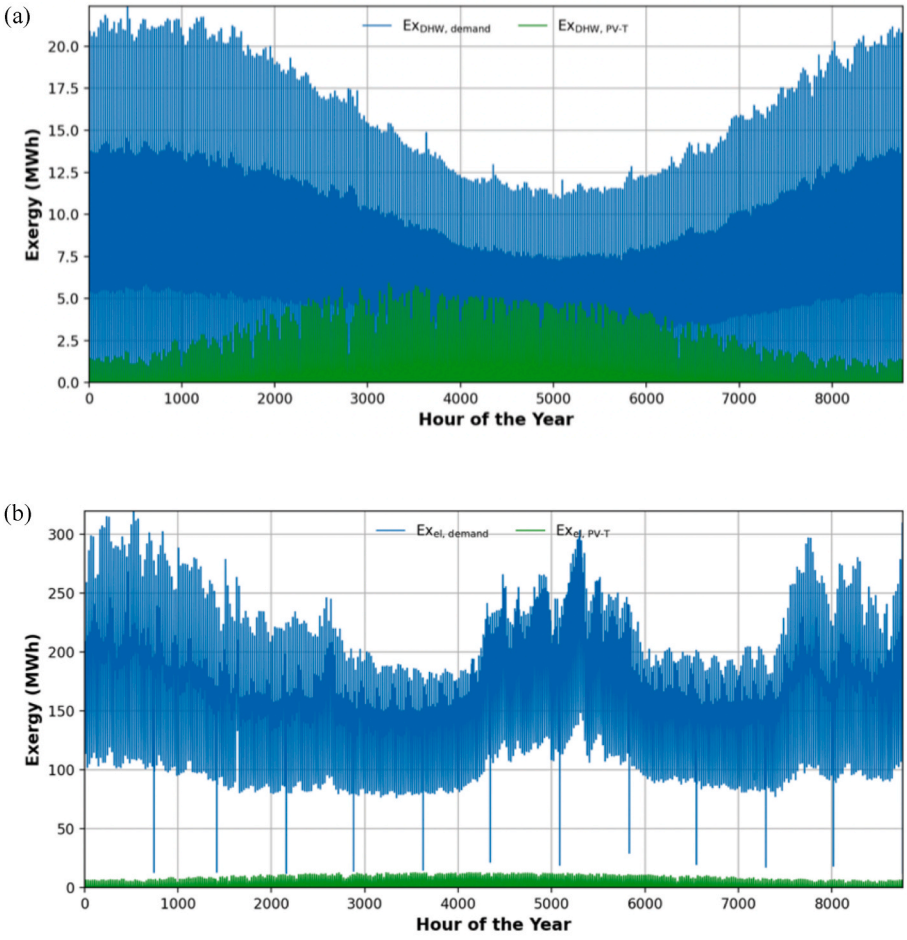


Fig. 7. Annual hourly profiles of the aggregated (a) DHW exergy demand and DHW exergy supplied by the PV-T collectors, (b) Electrical exergy demand and electrical exergy supplied by the PV-T collectors, across Tarragona province.

demand. These energy outputs align well with the findings of the computational study by Penaka et al. [55]. The authors reported annual thermal and electrical outputs of *881.6 kWh$_{th}$/m^2/yr* and *244 kWh$_e$/-m^2/yr, respectively,* for a water-based PV-T collector at Barcelona (Spain) which is a location with climatic condition similar to those of Tarragona province. This further confirms the reliability of the model in the study in predicting PV-T collector performance under similar environmental conditions.

3.6. Economic viability and profitability of the PV-T collector installations

To streamline the presentation, the results of the economic assessment of the proposed PV-T collector installations were aggregated at the provincial level, following the initial calculations made for individual municipalities.

Fig. 8 illustrates the projected cumulative cash flows for the PV-T collector installations over a 20-year period. These cash flows were derived by discounting the expected financial savings and the operation and maintenance (O&M) costs, relative to the capital investment for each year. The total capital investment for the PV-T collectors and installations amounted to approximately *52.12 M€* resulting in an average capital cost of about *575.10 €/m^2* (ranging from *575.00 €/m^2* to *596.34 €/m^2*). This translated to an average capital investment budget of about 71.89 €/capita (ranging from *71.88 €/capita* to *74.54 €/capita*). The total annual O&M was about 1.29 M€, which equated to an average of *12.5 €/m^2* or approximately *1.56 €/capita*. These figures indicate that the proposed PV-T installations are affordable within the municipalities.

The initial total annual financial savings expected from the PV-T collector installations across the province amount to approximately *12.84 M€* (*~117.81 – 130.80 €/m^2/annum*), representing about *20.83 %* (*~18.59 – 22.19 %)* of the total annual costs for DHW energy and electricity consumption in the province. Fig. 8 shows a linear increase in the cumulative cash flow from the installations, from the end of the year of installation (Year 0) until the end of life (Year 19). A noticeable slowdown in the growth occurred in Year 9, primarily due to the cost of replacing the electrical inverters. The mean payback period of the initial total investment was achieved in Year 5. However, the payback varied across municipalities: only about *15.7 %* of the municipalities recovered their investment by Year 5, while the remaining *84.3 %* achieved payback by Year 6. After this point, despite ongoing annual O&M costs, the PV-T installations continue to generate positive savings in all the municipalities for the rest of their operational lives. By Year 19, the Net Present Value (NPV) of the installations aggregated across all municipalities was approximately *168.1 M€*, with a mean of *1633.04 €/m^2* (ranging from 1485.82 €/m^2 to 1755.86 €/m^2). These results demonstrate that the proposed rooftop PV-T collector installations are both economically viable and profitable in all the municipalities across the province.

Fig. 9 presents the box plot illustrating the Levelized Cost of Exergy (LCOEx) for the PV-T collector installations over their lifetimes. The LCOEx ranged from *8.43 c€/kWh* to *9.95 c€/kWh*, with a mean value of approximately *8.95 c€/kWh*. These costs are comparable to the current cost of natural gas (*~8.91 c€/kWh*) and lower than the current hourly electricity prices, indicating a competitive economic performance for the PV-T installations.

3.7. Equivalent CO_2 emission mitigation

The environmental analysis, as shown in Fig. 10, reveals that the proposed PV-T collector installations could mitigate 20.8 % (*23.83 ktCO$_2$-eq*) of the annual CO_2 emissions associated with domestic hot water (DHW) consumption in Tarragona province (baseline: *303.78 ktCO$_2$-eq*). This mitigation potential varied across the municipalities, ranging from 18.6 % to 22.2 %. In addition, the PV-T collector installations would reduce electricity-related emissions (baseline: *303.78*

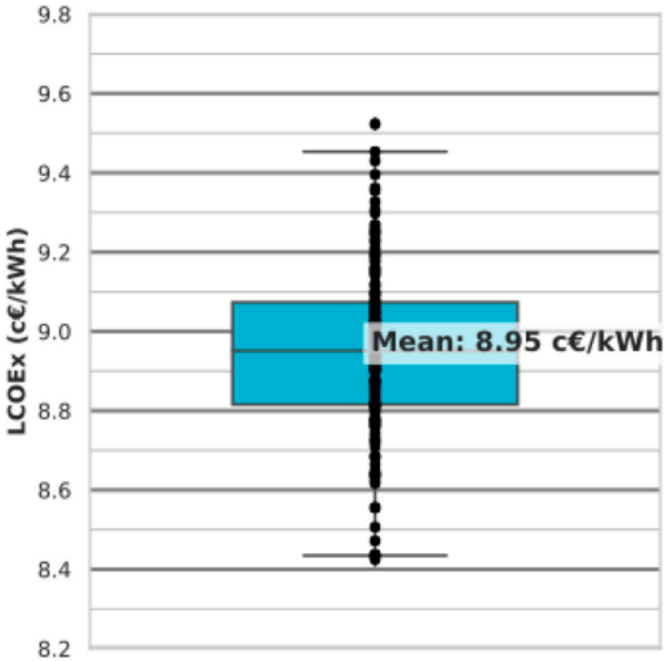


Fig. 9. A box plot of the Levelized Cost of Exergy (LCOEx) realized from the PV-T collector installations in all the municipalities of Tarragona province.

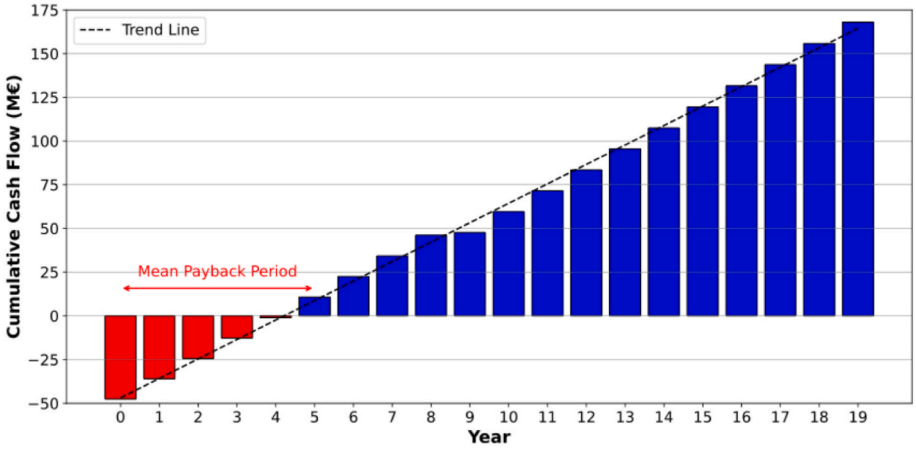


Fig. 8. Cumulative cashflow from the rooftop PV-T collector installations in Tarragona province aggregated annually from the constituent municipalities.

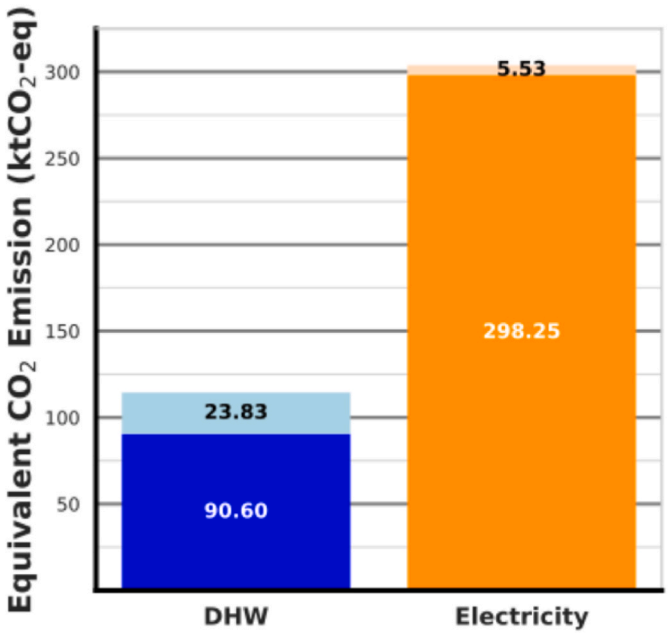


Fig. 10. A chart of the aggregated annual masses of equivalent CO_2 emissions associated with the consumption of DHW and electricity in Tarragona province and the potential equivalent CO_2 emissions that would be avoided by the PV-T installations (in lighter shades).

$ktCO_2$-eq) by *1.8 %* (*5.53 $ktCO_2$-eq*) annually, with municipal variability ranging from *0.1 %* to *7.7 %*. Collectively, the proposed installations would offset *7.02 %* (*~29.3 $ktCO_2$-eq*) of the province's combined DHW and electricity annually. When normalized by PV-T collector area, this equates to a mean CO_2 emissions avoidance potential of approximately *285.6 $kgCO_2$-eq/m^2/yr* (ranging: *269.6 – 299.4 $kgCO_2$-eq/m^2/annum*). This demonstrates the significant decarbonization potential of the proposed installations for the province.

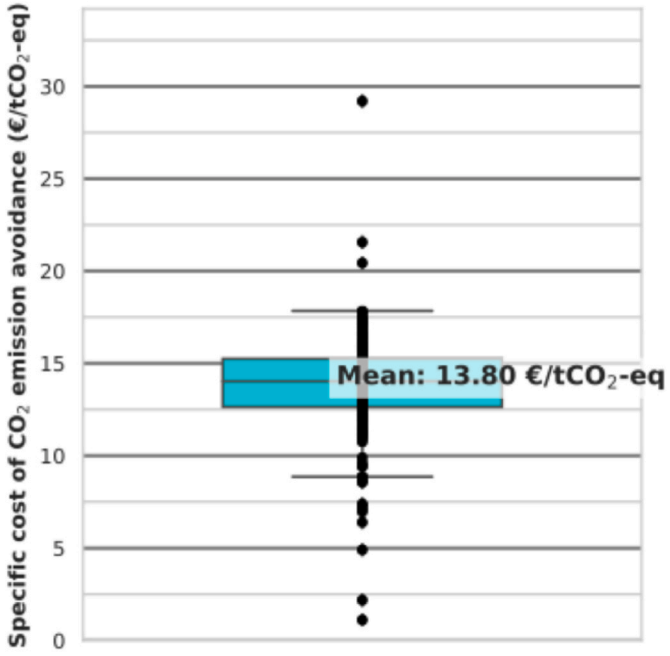


Fig. 11. A box plot of the Specific cost of CO_2 avoidance offered by the proposed PV-T collector installations across the municipalities in Tarragona province.

Fig. 11 presents the specific cost of equivalent CO_2 emissions avoidance offered by the PV-T collector installations across Tarragona province. The mean cost of equivalent CO_2 emissions avoidance over system's 20-year lifetime is *13.80 €/tCO_2-eq*, with a wide variation across municipalities ranging from *1.12* to *29.21 €/tCO_2-eq* across the municipalities. This variability can be attributed to several factors such as: (1) the deployment scale, where larger installations in more populous municipalities benefit from economies of scale, (2) differences in energy demand due to varying DHW and electricity consumption profiles, and (3) meteorological conditions, such as variations in solar irradiance and the ambient temperature gradients.

3.8. Comparison with conventional rooftop solar technologies from literature

The results of this study were benchmarked against conventional rooftop solar configurations reported in literature, as summarized in Table 7. The comparative analysis highlights the superior energetic, economic, and environmental performance of the proposed PV-T collectors' configuration under the prevailing climatic conditions in the study area.

In terms of energy output, the proposed PV-T collectors' configuration in this current study presents higher annual energy generation exceeding those of the rooftop PV-only system in Italy [56] and the PV-T + heat pump system in the UK [58].

Even the rooftop solar thermal system in China [57], despite the use of thermal storage, produced a lower thermal energy output. The efficiency metrics further reinforce this trend, as the proposed configuration in this present study operated at both higher PV and thermal efficiencies than both the flat-plate solar thermal system [57] and the hybrid system [58].

Economically, the proposed PV-T configuration in this study is the most viable option, with Levelized Cost of Exergy (LCOEx) from *0.08* to *0.09 €/kWh* and a payback period of just *5–6* years. This is notably shorter than the payback times reported for PV in Italy (*8.26* years), flat-plate solar thermal collector with storage in China (*15.8* years), and the hybrid PV-T collector with heat pump system in the UK (*14* years), all of which also had higher LCOEx values.

From an environmental perspective, the estimated average annual CO_2 emissions savings obtained by the configuration in this study far exceed those reported in the other studies considered.

These comparisons (summarized in Table 7) validate the strong performance of the proposed configuration across multiple dimensions, energetic, economic, and environmental. This is even with its simplified design features and lack of energy storage. Unlike conventional PV-T systems that often incorporate thermal energy storage tanks, electrical batteries, and active control systems, the proposed configuration uses passive, storage-free layout with constant water flow. This reduces capital costs, simplifies installation, and minimizes maintenance, while achieving shorter payback payback periods (*5–6 years*) and lower LCOEx (*0.08 - 0.09 €/kWh*) than more complex alternatives like the PV-T/heat pump system in the UK [58]. Despite the absence of auxiliary subsystems, it maintains high thermal and electrical efficiencies, and its replicability and scalability for community-scale deployment in other regions aiming for affordable and impactful energy decarbonization in the residential sector.

3.9. Sensitivity analysis of key input parameters

To evaluate the robustness of the techno-economic outcomes of the PV-T collector installations in Tarragona province, a sensitivity analysis was conducted by aggregating the performance results across all the *184* municipalities. The analysis evaluated the influences of six key input parameters: solar irradiation, electricity price, natural gas price, capital cost, the CO_2 emission factor for electricity, and the CO_2 emission factor for natural gas. Each parameter was independently varied by *±5 %* and

Table 7
Comparison of the current study with other rooftop solar technologies in literature.

Reference	Metric				
	Energy Output (*kWh/m²/yr*)	Efficiency (%)	Payback Period (*years*)	LCOEx (*€/kWh*)	CO_2 Savings (tCO_2-eq/m^2/yr)
Current study	233.0–259.6 (PV) + 808.4–896.9 (Thermal)	14.4–14.6 % (PV) + 48.6–50.7 % (Thermal)	5–6	0.08–0.09	5.44 (Aggregated for the province)
Rooftop PV (Italy) [56]	224.0 (PV)	11.6 % (PV)	8.26	0.15	0.06
Rooftop Flat-plate Thermal Collector + Storage (China) [57]	565.3 (Thermal)	30.0 % (Thermal)	15.8	0.099	0.31
Rooftop PV-T + Heat Pump (United Kingdom) [58]	164.7 (PV) + 123.0 (Thermal)	15.6 % (PV) + 13.1 % (Thermal)	14	0.20	0.06

±*10 %* relative to its baseline value (set at *0 %*), while all others were held constant. This approach facilitated an assessment of how changes in climatic, economic, and technological conditions could influence the four core performance indicators: annual solar fraction, net present value (NPV), payback period, and CO_2 emission reduction, all computed for the entire province. Fig. 12 presents a heatmap visualization of the percentage change in each output metric in response to these variations, clearly illustrating the direction and magnitude of impacts, thus aiding interpretation of parameter sensitivity.

The analysis revealed that solar irradiation had the most comprehensive and pronounced effect across all performance indicators. Increase in solar irradiation led to proportional improvements in solar fraction, NPV, and CO_2 emission reductions, while simultaneously shortening the payback period. This trend underscores the system's strong dependence on solar resource intensity, as both thermal and electrical outputs are directly proportional to available sunlight.

Electricity and natural gas prices were the key economic drivers, particularly influencing the NPV and the payback period. Higher energy prices improved economic performance by increasing the value of displaced utility consumption, although they had no influence on solar fraction or CO_2 emissions. This highlights the critical role that energy market pricing plays in determining system's profitability. Conversely, capital cost influenced only economic metrics, with its reductions resulting in better NPV and shorter payback periods, while energy outputs and emissions remained unaffected. This observation emphasizes the importance of technological cost reductions and financial incentives in driving the adoption of PV-T systems.

CO_2 emission factors for electricity and natural gas primarily influenced environmental performance, particularly the emissions offset by PV-T deployment. The equivalent CO_2 emission reduction was more sensitive to variations in the natural gas emission factor, reflecting the high share of thermal energy contribution from the PV-T collectors in domestic hot water production.

Variations in the CO_2 emission factor for electricity had a more modest impact, suggesting that as the national electricity grid decarbonizes, the marginal emissions benefit of electricity generated by the collectors may gradually diminish.

In summary, the sensitivity analysis revealed distinct influence pathways for each parameter. Solar irradiation and energy prices drive

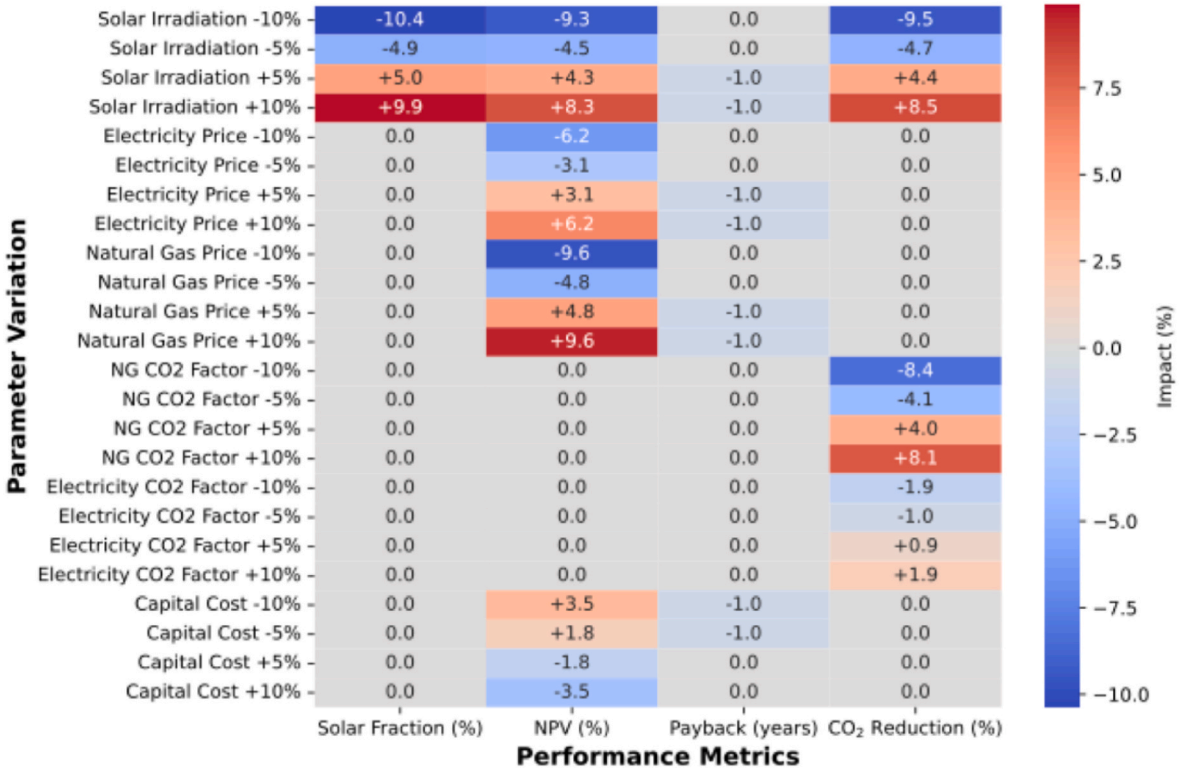


Fig. 12. Heatmap of parameter variation effects on selected performance metrics (payback in actual change in years).

both environmental and financial outcomes, while capital cost determines the economic feasibility. Emission factors play key roles in shaping the environmental impact mitigation. These insights are crucial for regional energy planners and policymakers aiming to promote large-scale deployment of PV-T collectors. They suggest that initiatives targeted at optimizing energy market structures, reducing technology costs, and enhancing accessibility to the solar energy technologies can substantially enhance the overall decarbonization potential of rooftop PV-T systems.

4. Conclusion

This study explored the large-scale deployment of water-based photovoltaic-thermal (PV-T) collectors on rooftops of residential buildings, providing a comprehensive assessment of their technical, economic, and environmental feasibility. By eliminating the need for auxiliary storage tanks and electrical battery, this approach significantly reduced upfront costs while maintaining strong performance metrics. The computational framework introduced in this study was applied to a real case study of Tarragona province, Spain, which includes 184 distinct municipalities. The province is characterized by Mediterranean climatic conditions and abundant solar resources.

The key findings from the case study indicate that the PV-T collectors provided annual outputs ranging from *808.4* to *896.9* kWh_{th}/m^2 for domestic hot water (DHW) and *233.0* to *259.6* kWh_e/m^2 for electricity. The average rooftop space required for PV-T installation was *0.125* m^2 per capita, occupying only *3.85 %* of the useable residential rooftop area across the province. The PV-T collectors would supply *11.8 %* of the exergy required for domestic hot water and *1.8 %* of the electricity demand, with an overall solar fraction of *2.2 %*.

The economic evaluation showed a payback period of *5–6* years and a net present value (NPV) of *1485.82 - 1755.86* €/m^2, with a levelized cost of exergy (LCOEx) ranging from *8.43* to *9.95* c€/*kWh*. The systems offered significant environmental benefits, mitigating *29.3* $ktCO_2$-*eq/year*, with a specific cost of equivalent CO_2 emission avoidance of *13.50* €/tCO_2-*eq*.

The study also highlights that the simplified design, which uses a constant water flow rate, led to very minimal annual thermal exergy losses (averaging *7.7 %* province-wide). These losses are relatively low and, in the context of the system's overall performance, have negligible impact on the feasibility of the proposed system. The ability of the PV-T collectors' configuration to generate significant energy with minimal additional components confirms its cost-effectiveness and energy efficiency, demonstrating beneficial life cycle performance. It should however be noted that considerable thermal exergy losses may be incurred if a significant number of the population in a community deviate from the hourly hot water demand profile adopted.

The sensitivity analysis conducted in this study revealed that variations in solar irradiation had the most significant impact on all performance metrics, impacting both environmental and economic outcomes. Additionally, higher electricity and natural gas prices further enhanced economic performance. The results also showed that capital costs significantly influenced economic viability, with reduced capital costs leading to better net present value (NPV) and shorter payback periods. Notably, the proposed PV-T collectors configuration demonstrated a comparatively lower LCOEx relative to some other rooftop solar energy technologies, which is a key factor in its attractiveness for widespread adoption. Government incentives aimed at reducing capital costs would accelerate the deployment of PV-T systems, making this technology more accessible and fostering large-scale adoption. This configuration offers significant advantages over other conventional PV-T configuration, by achieving outstanding energy performance and faster payback of initial financial investment, while reducing system's complexity and cost.

Despite the promising results, practical challenges exist, particularly regarding the integration of PV-T collectors into existing residential energy systems. Factors such as the need of retrofitting older buildings, and possible rooftop space limitations on some individual buildings may impact the practicality of deployment. Consumer behavior, including willingness to invest in renewable technologies and adapt to new systems, is also an important factor that could influence the adoption rate of PV-T systems. Further research is needed to address these challenges, including exploring dynamic water flow controls, minimal thermal energy storage options, and other strategies for improving energy self-consumption within communities. A suitable dynamic water control strategy would mitigate potential water overheating during periods of higher-than-typical solar irradiation. Furthermore, long-term experimental studies of water-based PV-T collectors, particularly in location of interest, would be essential to verify the projected performance and validate the system's real-world operational efficiency. Such studies, which are currently limited, are necessary to further refine the system's design and enhance its practical applicability.

Finally, the configuration introduced in this study provides a promising opportunity for the development of renewable energy communities, where households can share both thermal and electrical energy generated by the PV-T systems. This model would not only contribute to increased energy self-sufficiency but also help to prevent energy wastage by optimizing energy usage within a community. By enabling such energy sharing, there would be reduction in the reliance on conventional sources, making the deployment of PV-T collectors even more cost-effective and efficient.

In conclusion, the findings of this study highlight the significant potential of large-scale deployment of PV-T collectors as a cost-effective, scalable solution for decarbonizing the residential energy sector. The proposed framework offers a valuable tool for accelerating the adoption of PV-T technology in other regions with similar climate and energy use profiles, making it a promising pathway toward achieving global energy transition goals.

CRediT authorship contribution statement

Adedamola B. Shobo: Writing – original draft, Visualization, Validation, Methodology, Investigation, Funding acquisition, Formal analysis, Data curation, Conceptualization. **Raul Saez:** Writing – review & editing, Validation, Funding acquisition, Data curation. **Dieter Boer:** Writing – review & editing, Supervision, Resources, Project administration, Funding acquisition. **Manel Vallès:** Writing – review & editing, Supervision, Resources, Project administration, Funding acquisition.

Declaration of competing interest

The authors declare the following financial interests/personal relationships which may be considered as potential competing interests: Adedamola B. Shobo reports financial support was provided by European Union. Adedamola B. Shobo reports financial support was provided by Generalitat de Catalunya Ministry of Research and Universities. Adedamola B. Shobo reports financial support was provided by Spain Ministry of Science and Innovation. Raul Saez reports financial support was provided by Generalitat de Catalunya Ministry of Research and Universities. Dieter Boer reports financial support was provided by Generalitat de Catalunya Ministry of Research and Universities. Manel Valles reports financial support was provided by Generalitat de Catalunya Ministry of Research and Universities. If there are other authors, they declare that they have no known competing financial interests or personal relationships that could have appeared to influence the work reported in this paper.

Acknowledgements

The authors would like to acknowledge financial support from the "Agència de Gestió d'Ajuts Universitaris i de Recerca (AGAUR)" from "Generalitat de Catalunya" (2022-FISDU-00128); the "Ministerio de Ciencia,

Innovaci'onyUniversidades"ofSpain(PID2021-127713OA-I00,PID2021-123511OB-C33, PID2021-124139NB-C22 [MICIU/AEI/10.13039/501100011033/FEDER, UE] & TED2021-129851B-I00 [MICIU/AEI/10.13039/501100011033/Uni'on Europea NextGenerationEU/PRTR]); and "Universitat Rovira i Virgili" in Spain (2021URV-MZ-11 Zambrano grant FundedbytheEuropeanUnion– NextGenerationEU).

Nomenclature

A_c	area of collector, m^2
c_w	specific heat capacity of water, $J/kg\,^oC$
$C_{Capital}$	capital investment, $€$
$C_{O\&M}$	cost of operation and management, $€$
d	discount rate,
e	annual energy price escalation rate,
$E_{DHW,demand}$	domestic hot water energy demand, J or kWh
$E_{el,PVT}$	electrical energy generated by PV-T collector, kWh
$E_{th,PVT}$	thermal energy generated by PV-T collector, kWh
$Ex_{DHW,PVT}$	useful thermal exeergy for domestic hot water from PV-T collector (kWh)
$Ex_{el,demand}$	electrical exergy demand, kWh
EP	electricity purchase price, $€/kWh$
ES	electricity selling price, $€/kWh$
F'	PV-T collector's thermal efficiency factor
F_R	PV-T collector's heat removal factor
G	Solar irradiance, W/m^2
GP	natural gas price, $€/kWh$
i	national interest rate
h	hour
$\dot{m}_w$	mass flow rate of water, kg/s
$NOCT_{PVT}$	nominal operating cell temperature of PV module
Pop	municipal population
R_y	annual monetary savings, $€$
T_a	ambient temperature, ^oC
$T_{a,avg}$	annual average ambient temperature, ^oC
$T_{a,max}$	maximum avarage monthly ambient temperature, ^oC
$T_{a,min}$	minimum avarage monthly ambient temperature, ^oC
T_{out}	temperature of water at PV-T collector outlet, ^oC
T_{PV}	temperature of PV module, ^oC
T_{STC}	temperature of PV module at stanndard testing conditions, ^oC
T_w	temperature of municipal water supply, ^oC
U_L	PV-T collector's overall heat loss coefficient, $W/m^2 \cdot K$
y	year number
Greek symbols	
γ	temperature coefficient of PV collector, $\%/^oC$
η_o	optical efficiency of PV-T collector glass cover
$\eta_{el,PVT}$	electrical efficiency of PV module inside collector
η_{STC}	electrical efficiency of PV module at standard testing conditions
ρ_w	Density of water, kg/m^3

References

[1] IEA, Energy Efficiency 2023, IEA, Paris, 2023. https://www.iea.org/reports/energy-efficiency-2023. (Accessed 14 December 2023). https://iea.blob.core.windows.net/assets/dfd9134f-12eb-4045-9789-9d6ab8d9fbf4/EnergyEfficiency2023.pdf. License: CC BY 4.0.

[2] M. Herrando, G. Fantoni, A. Cubero, R. Simón-Allué, I. Guedea, N. Fueyo, Numerical analysis of the fluid flow and heat transfer of a hybrid PV-thermal collector and performance assessment, Renew. Energy 209 (2023) 122–132, https://doi.org/10.1016/j.renene.2023.03.125.

[3] Y. Elomari, C. Mateu, M. Marín-Genescà, D. Boer, A data-driven framework for designing a renewable energy community based on the integration of machine learning model with life cycle assessment and life cycle cost parameters, Appl. Energy 358 (2024) 122619, https://doi.org/10.1016/j.apenergy.2024.122619.

[4] H.H. Pourasl, R.V. Barenji, V.M. Khojastehnezhad, Solar energy status in the world: a comprehensive review, Energy Rep. 10 (2023) 3474–3493, https://doi.org/10.1016/j.egyr.2023.10.022.

[5] X. Liao, R. Zhu, M.S. Wong, J. Heo, P.W. Chan, C.Y.T. Kwok, Fast and accurate estimation of solar irradiation on building rooftops in Hong Kong: a machine learning-based parameterization approach, Renew. Energy 216 (2023) 119034, https://doi.org/10.1016/j.renene.2023.119034.

[6] A.K. Hamzat, A.Z. Sahin, M.I. Omisanya, L.M. Alhems, Advances in PV and PVT cooling technologies: a review, Sustain. Energy Technol. Assessments 47 (2021) 101360, https://doi.org/10.1016/j.seta.2021.101360.

[7] M. Emam, A. Hamada, H.A. Refaey, M. Moawed, M.A. Abdelrahman, M.R. Rashed, Year-round experimental analysis of a water-based PVT-PCM hybrid system: comprehensive 4E assessments, Renew. Energy 226 (2024) 120354, https://doi.org/10.1016/j.renene.2024.120354.

[8] M. Herrando, A. Ramos, I. Zabalza, Cost competitiveness of a novel PVT-based solar combined heating and power system: influence of economic parameters and financial incentives, Energy Convers. Manag. 166 (2018) 758–770, https://doi.org/10.1016/j.enconman.2018.04.005.

[9] F. Huide, Z. Xuxin, M. Lei, Z. Tao, W. Qixing, S. Hongyuan, A comparative study on three types of solar utilization technologies for buildings: photovoltaic, solar thermal and hybrid photovoltaic/thermal systems, Energy Convers. Manag. 140 (2017) 1–13, https://doi.org/10.1016/j.enconman.2017.02.059.

[10] M. Herrando, K. Wang, G. Huang, T. Otanicar, O.B. Mousa, R.A. Agathokleous, Y. Ding, S. Kalogirou, N. Ekins-Daukes, R.A. Taylor, C.N. Markides, A review of solar hybrid photovoltaic-thermal (PV-T) collectors and systems, Prog. Energy Combust. Sci. 97 (2023) 101072, https://doi.org/10.1016/j.pecs.2023.101072.

[11] S. Abdul-Ganiyu, D.A. Quansah, E. Ramde, R. Seidu, M.S. Adaramola, Techno-economic analysis of solar photovoltaic (PV) and solar photovoltaic thermal (PVT) systems using exergy analysis, Energy Technol. 47 (Assessments 2021) 101520, https://doi.org/10.1016/j.seta.2021.101520.

[12] M. Hazami, A. Riahi, F. Mehdaoui, O. Nouicer, A. Farhat, Energetic and exergetic performances analysis of a PV/T (photovoltaic thermal) solar system tested and simulated under to Tunisian (North Africa) climatic conditions, Energy 107 (2016) 78–94, https://doi.org/10.1016/j.energy.2016.03.134.

[13] A. Behzadi, A. Arabkoohsar, Y. Yang, Optimization and dynamic techno-economic analysis of a novel PVT-based smart building energy system, Appl. Therm. Eng. 181 (2020) 115926, https://doi.org/10.1016/j.applthermaleng.2020.115926.

[14] J.A. Aguilar-Jiménez, L. Hernández-Callejo, V. Alonso-Gómez, N. Velázquez, R. López-Zavala, A. Acuña, D. Mariano-Hernández, Techno-economic analysis of hybrid PV/T systems under different climate scenarios and energy tariffs, Sol. Energy 212 (2020) 191–202, https://doi.org/10.1016/j.solener.2020.10.079.

[15] María Herrando, Daniel Elduque, Carlos Javierre, Norberto Fueyo, Life Cycle Assessment of solar energy systems for the provision of heating, cooling and electricity in buildings: a comparative analysis, Energy Convers. Manag. 257 (2022) 115402, https://doi.org/10.1016/j.enconman.2022.115402.
[16] Ehsan Karkon, Mohammad Liravi, Laurent Georges, Jinping Li, Vojislav Novakovic, Design of a hybrid solar and biomass-based energy system integrated with near-zero energy building: Techno-environment investigation and multicriteria optimization, Process. Saf. Environ. Prot. 193 (2025) 26–42, https://doi.org/10.1016/j.psep.2024.11.018.
[17] A.I. Osman, L. Chen, M. Yang, G. Msigwa, M. Farghali, S. Fawzy, D.W. Rooney, P.-S. Yap, Cost, environmental impact, and resilience of renewable energy under a changing climate: a review, Environ. Chem. Lett. 21 (2023) 741–764, https://doi.org/10.1007/s10311-022-01532-8.
[18] A. Parreño-Rodriguez, A.P. Ramallo-González, M. Chinchilla-Sánchez, A. Molina-García, Community energy solutions for addressing energy poverty: a local case study in Spain, Energy Build. 296 (2023) 113418, https://doi.org/10.1016/j.enbuild.2023.113418.
[19] R. Saez, D. Boer, A.B. Shobo, M. Vallès, Techno-economic analysis of residential rooftop photovoltaics in Spain, Renew. Sustain. Energy Rev. 188 (2023) 113788, https://doi.org/10.1016/j.rser.2023.113788.
[20] Adedamola Shobo, Raul Saez, Youssef Elomari, Dieter Boer, Manel Valles, Ruslan Kotegov. Techno-economic analysis of rooftop photovolataic-thermal collectors' installations in residential energy communities. In Proceedings of the 37th International Conference on Efficiency, Cost, Optimization, Simulation and Environmental Impact of Energy Systems (ECOS 2024), Rhodes, Greece:2125-2136. https://doi.org/10.52202/077185-0182.
[21] M.J. Wolf, J.W. Emerson, D.C. Esty, A. de Sherbinin, Z.A. Wendling, et al., 2022 Environmental Performance Index, Yale Center for Environmental Law & Policy, New Haven, CT, 2022. https://epi.yale.edu/about-epi. (Accessed 8 January 2024).
[22] Ministerio para la Transición Ecológica y el Reto Demográfico, Plan nacional Integrado de Energía y Clima (PNIEC) 2021-2030 (2020). https://www.miteco.gob.es/es/ministerio/planes-estrategias/plan-nacional-integradoenergia-clima/plannacionalintegradodeenergiayclima2021-2030_tcm30-546623.pdf. (Accessed 24 April 2024).
[23] M. García-López, B. Montano, J. Melgarejo, Household energy consumption and the financial feasibility of self-consumption through photovoltaic panels in Spain, Energ Effic 16 (2023) 57, https://doi.org/10.1007/s12053-023-10139-z.
[24] Red Eléctrica, Energy from the sun: installed capacity, photovoltaic solar. https://www.sistemaelectrico-ree.es/en/renewable-energies-report/sun/installed-capacity/photovoltaic-solar-sunpower. (Accessed 15 January 2024).
[25] I. Mariuzzo, D. Fioriti, E. Guerrazzi, D. Thomopulos, M. Raugi, Multi-objective planning method for renewable energy communities with economic, environmental and social goals, Int J Elec Power 153 (2023) 109331, https://doi.org/10.1016/j.ijepes.2023.109331.
[26] Asociación de Empresas Eléctricas (ASEME) DATADIS, La plataforma de datos de consumo eléctrico. https://datadis.es/home, 2022. (Accessed 11 January 2024).
[27] Instituto Nacional de Estadística (INE), Municipal register. https://www.ine.es/dyngs/INEbase/en/categoria.htm?c=Estadistica_P&cid=1254734710990, 2023. (Accessed 1 February 2023).
[28] European Commission JRC photovoltaic geographical information system (PVGIS). https://re.jrc.ec.europa.eu/pvg_tools/en/, 2023. (Accessed 2 February 2023).
[29] Ministry of Development, Estudio (01) para la ERESEE 2020 "Estrategia a largo plazo para la Rehabilitación Energética en el Sector de la Edificación en España". https://cdn.mitma.gob.es/portal-webdrupal/planes_estartegicos/1_2020_segmentacion_parque_residencial_clusteres.pdf. (Accessed 17 January 2024).
[30] Institut d'Estadística de Catalunya, Habitatges (Fins al 2021). https://www.idescat.cat/pub/?id=censph&n=16993. (Accessed 1 May 2024).
[31] J. Arcas-Abella, A. Pagès-Ramon, E. Larrumbide, D. Huerta, Segmentación del parque residencial de viviendas en España en clústeres tipológicos. https://cdn.mitma.gob.es/portal-web-drupal/planes_estartegicos/1_2020_segmentacion_parque_residencial_clusteres.pdf, 2019. (Accessed 30 April 2024).
[32] S. Izquierdo, M. Rodrigues, N. Fueyo, A method for estimating the geographical distribution of the available roof surface area for large-scale photovoltaic energy-potential evaluations, Sol. Energy 82 (2008) 929–939, https://doi.org/10.1016/j.solener.2008.03.007.
[33] Ministerio de Transportes, Movilidad y Agenda Urbana, Spain, Documento Básico HE – Ahorro de energía. https://www.codigotecnico.org/pdf/Documentos/HE/DcmHE.pdf, 2022. (Accessed 18 January 2024).
[34] V. Sun, A. Asanakham, T. Deethayat, T. Kiatsiriroat, Evaluation of nominal operating cell temperature (NOCT) of glazed photovoltaic thermal module, Case Stud. Therm. Eng. 28 (2021) 101361, https://doi.org/10.1016/j.csite.2021.101361.
[35] Powervolt | solimpeks solar corp. http://www.solimpeks.com/product/volther-powervolt/, 2016.
[36] Maurizio Cellura, Quyen Luu Le, Francesco Guarino, Sonia Longo, A review on life cycle environmental impacts of emerging solar cells, Sci. Total Environ. 908 (2024) 168019, https://doi.org/10.1016/j.scitotenv.2023.168019.
[37] M. Lämmle, A. Oliva, M. Hermann, K. Kramer, W. Kramer, PVT collector technologies in solar thermal systems: a systematic assessment of electrical and thermal yields with the novel characteristic temperature approach, Sol. Energy 155 (2017) 867–879, https://doi.org/10.1016/j.solener.2017.07.015.
[38] K. Ilse, L. Micheli, B.W. Figgis, K. Lange, D. Daßler, H. Hanifi, F. Wolfertstetter, V. Naumann, C. Hagendorf, R. Gottschalg, J. Bagdahn, Techno-Economic assessment of soiling losses and mitigation strategies for solar power generation, Joule 3 (10) (2019) 2303–2321, https://doi.org/10.1016/j.joule.2019.08.019.
[39] A. Gagliano, G.M. Tina, S. Aneli, S. Nižetić, Comparative assessments of the performances of PV/T and conventional solar plants, J. Clean. Prod. 219 (2019) 304–315, https://doi.org/10.1016/j.jclepro.2019.02.038.
[40] Statista – Harmonized index of consumer prices (HICP) energy inflation rate in Spain from January 2019 to May 2023, by commodity. https://www.statista.com/statistics/1329221/spain-energy-inflation-rate-by-commodity/(Accessed 19. January.2024).
[41] Eurostat, Gas prices for household consumers - bi-annual data (from 2007 onwards). https://ec.europa.eu/eurostat/databrowser/view/NRG_PC_202/default/table?lang=en (Accessed 1.February.2024).
[42] Statista - Spain: inflation rate from 1987 to 2028. https://www.statista.com/statistics/271077/inflation-rate-in-spain/(Accessed 4.December.2023).
[43] Statista – Carbon intensity of the power sector in Spain from 2000 to 2022. https://www.statista.com/statistics/1290486/carbon-intensity-power-sector-spain/#:~:text=In%202022%2C%20Spain%27s%20power%20sector,up%20from%20the%20previous%20year (Accessed 26.September.2023).
[44] H. Lin, J. Clavreul, C. Jeandaux, J. Crawley, I. Butnar, Environmental life cycle assessment of heating systems in the UK: comparative assessment of hybrid heat pumps vs. condensing gas boilers, Energy Build. 240 (2021) 110865, https://doi.org/10.1016/j.enbuild.2021.110865.
[45] Hendron R, Anderson R, Christensen C. Eastment M., Development of an energy savings benchmark for all residential end-uses. Proceedings of SIMBUILD2004 Conference, Colorado :1-11. https://www.nrel.gov/docs/fy04osti/35917.pdf.
[46] M. Żukowski, Experimental determination of the cold water temperature at the inlet to solar water storage tanks, Therm. Sci. Eng. Prog. 16 (2020) 100466, https://doi.org/10.1016/j.tsep.2019.100466.
[47] P. Carnero, P. Calatayud, A parametric analysis for short-term residential electrification with electric water tanks. The case of Spain, Sustainability 13 (21) (2021) 12070, https://doi.org/10.3390/su132112070.
[48] D. Leiria, H. Johra, A. Marszal-Pomianowska, M.Z. Pomianowski, A methodology to estimate space heating and domestic hot water energy demand profile in residential buildings from low-resolution heat meter data, Energy 263 (B) (2023) 125705, https://doi.org/10.1016/j.energy.2022.125705.
[49] American Society of Heating, Refrigerating and Air-Conditioning Engineers, ASHRAE handbook—Hvac Applications, SI ed., ASHRAE, Atlanta, GA, 2015.
[50] O.R. Alomar, O.M. Ali, Energy and exergy analysis of hybrid photovoltaic thermal solar system under climatic condition of North Iraq, Case Stud. Therm. Eng. 28 (2021) 101429, https://doi.org/10.1016/j.csite.2021.101429.
[51] L. Micheli, F.A. Sepúlveda-Vélez, D.L. Talavera, Impact of variable economic conditions on the cost of energy and the economic viability of floating photovoltaics, Heliyon 10 (12) (2024) e32354, https://doi.org/10.1016/j.heliyon.2024.e32354.
[52] H.L. Azeez, A. Ibrahim, J. Kasprzak, B.O. Ahmed, A.H.A. Al-Waeli, M. Jaber, Economic and environmental feasibility analysis of a photovoltaic thermal system with passive cooling techniques, nanofluid, and phase changing materials, Appl. Therm. Eng. 274 (C) (2025) 126782, https://doi.org/10.1016/j.applthermaleng.2025.126782.
[53] L. Cabeza, Encyclopedia Energy Storage. Lleida, Spain, Elsevier, 2022.
[54] C.-H. Park, Y.-J. Ko, J.-H. Kim, H. Hong, Greenhouse gas reduction effect of solar energy systems applicable to high-rise apartment housing structures in South Korea, Energies 13 (10) (2020) 2568, https://doi.org/10.3390/en13102568.
[55] S.R. Penaka, P.K. Saini, X. Zhang, A. Amo, Digital mapping of techno-economic performance of a water-based solar Photovoltaic/Thermal (PVT) System for buildings over large geographical cities, Buildings 10 (9) (2020) 148, https://doi.org/10.3390/buildings10090148, 2020.
[56] Annarita Paiano, Giovanni Lagioia, Carlo Ingrao, A combined assessment of the energy, economic and environmental performance of a photovoltaic system in the Italian context, Sci. Total Environ. 866 (2023) 161329, https://doi.org/10.1016/j.scitotenv.2022.161329.
[57] E.B. Agyekum, T. Khan, N.C. Giri, Evaluating the technical, economic, and environmental performance of solar water heating System for residential applications–comparison of two different working fluids (water and glycol), Sustainability 15 (19) (2023) 14555, https://doi.org/10.3390/su151914555.
[58] Mustapha A. Obalanlege, Jingyuan Xu, Christos N. Markides, Yasser Mahmoudi, Techno-economic analysis of a hybrid photovoltaic-thermal solar-assisted heat pump system for domestic hot water and power generation, Renew. Energy 196 (2022) 720–736, https://doi.org/10.1016/j.renene.2022.07.044.